



Original article

Spectroscopic study of mixtures of green copper pigments in fresh and aged model samples. Case studies on masterpieces from the Spanish Golden Age

Carmen Paz^a, Luis-R. Rodríguez-Simón^b, Eloisa Manzano^{a,*}^a Department of Analytical Chemistry, University of Granada, Fuentenueva s/n, 18071 Granada, Spain^b Department of Paint and Restoration, University of Granada, Av. Andalucía n°38, 18071 Granada, Spain

ARTICLE INFO

Article history:

Received 19 July 2022

Accepted 14 December 2022

Available online 31 December 2022

Keywords:

μFTIR-ATR

μRS

Model samples

Alonso Cano

Green copper pigments

ABSTRACT

Precise knowledge of the palette employed by historic painters is fundamental to preserving their works of art and can help pinpoint the period in which their paintings were created, their provenance and authorship. Raman and IR spectroscopy is successful in identifying pigments via their molecular spectrum, nevertheless, to distinguish the pigments in a binary mixture is challenging, particularly when the mixed pigments are the same colour and Cu-containing. This is precisely the aim of the current research: to evaluate the effectiveness of the molecular spectroscopy techniques μRS and μFTIR-ATR to discriminate binary mixtures of three green pigments, all containing copper, specifically copper resinate, malachite and verdigris. To that end, two sets of model samples were prepared with pure pigments and their binary mixtures in variable weight concentrations from 20% to 80% for each component. The 15 model samples obtained were mixed with linseed oil in the fixed proportion of 3:1 (w/w) of powdered pigment to binder and spread in a homogeneous layer on a support of commercial grade canvas. Five replicates of μFTIR-ATR and μRS spectra, respectively, were recorded after 0 h, 24 h, 48 h, 72 h and 144 h of exposure within the controlled conditions of a climatic chamber. The aim is to establish the minimum percentage of a Cu-containing pigment in a binary mixture that can be detected by μRS and/or μFTIR-ATR spectroscopy. The product of this ample study is a database of the spectroscopic signature of each pigment in the specific mixtures (in the given proportions and artificial ageing times) for reference purposes in the study of the green areas of selected masterpieces. The oil paintings used in the research (*The Nativity*, *The Visitation*, and *The Assumption*) are of Alonso Cano's work, a well-known artist of the Spanish Golden Age (the *Siglo de Oro* in Spanish). With this study, the knowledge of the mixture of green pigments employed in Cano's palette was expanded, making considerable progress in the ambitious National Projects in which our Research Group, ever since 2003, has been attempting to understand Cano's technique.

© 2022 The Author(s). Published by Elsevier Masson SAS on behalf of Consiglio Nazionale delle Ricerche (CNR).

This is an open access article under the CC BY-NC-ND license (<http://creativecommons.org/licenses/by-nc-nd/4.0/>)

1. Research aim

It is widely known that artists very often use mixtures of pigments to achieve specific effects or tonal qualities, complicating the interpretation of the spectroscopic data. The research aim addressed in the present study concerns the effectiveness of molecular spectroscopy techniques, μRS and μFTIR-ATR, to discriminate pigments in binary mixtures even when one of the components

is in low proportion. The matter of pigment mixtures continues to be an analytical challenge particularly when the pigments are the same colour and Cu-containing. This is the specific area of the present work: binary mixtures of three historical green pigments, all containing copper, malachite, verdigris and copper resinate. The spectroscopic marker bands achieved were used for reference purposes to interpret the spectra acquired from the green-coloured areas of three selected easel paintings that Alonso Cano (Spanish Golden Age, 17th century) painted for the Main Chapel of the Granada cathedral (Spain). Additionally, the study established the minimum percentage necessary to be detected of any single pigment in the binary mixtures, helping clarify real sample misinterpretations.

* Corresponding author at: Department of Analytical Chemistry, University of Granada Faculty of Sciences, University of Granada, Fuentenueva s/n, 18071 Granada, Spain.

E-mail address: emanzano@ugr.es (E. Manzano).

2. Introduction

Cultural heritage materials such as murals, canvas paintings, polychrome and metal objects and paper artworks are complex multicomponent and multi-layered mixtures, with added complexity due to ageing. Scientific research in the interpretation of the composition of artistic materials is crucial in answering questions regarding the conservation, restoration, authorship, and authentication of works of art. This is the reason why this study focuses on one of the more prevalent materials used in artistic paintings: pigments. The green pigments selected for the study (malachite (M), verdigris (V) and copper resinate (CR)) are prevalent in historical documents and restoration manuals [1–4]. Verdigris is a green pigment composed of copper salts of acetic acid widely used in 15th and 16th century painting. It was also used in Ancient Greece (mentioned by Pliny in his *Naturalis Historia* in the Roman Age) as well as during the Middle Ages, the Renaissance and Baroque Period [5]. Malachite is perhaps the oldest known bright green pigment, the natural mineral basic copper carbonate. It was used as eye-paint since Predynastic times, in paintings throughout the Greek and Roman periods, then in European easel paintings in the 15th and 16th centuries. Malachite was also used in Western Chinese painting in the 10th and 11th centuries. Copper resinate is obtained by the dissolution of verdigris or copper acetate in an acidic resin such as colophony or Venice turpentine. It was commonly used during the later Middle Ages and Renaissance, but its use ceased in the 19th century because of its instability (change of its original colour). For the identification of these green pigments and other has been addressed in published research using techniques implemented in the present study such as Raman Spectroscopy (RS) [3,6–10] and Attenuated Total Reflection in conjunction with Fourier Transform Infrared Spectroscopy (μ FTIR-ATR) [11]. Many other techniques have been used in pigment identification such as Time-of-Flight Secondary Ion Mass Spectrometry (TOF-SIMS) [12], X-Ray Powder Diffraction (XRD) [13] and Hyperspectral Imaging (HSI) [14]. Nevertheless, given the notorious use of pigment mixtures by artists in search of pictorial effects or tonal qualities, the task of discriminating a specific pigment in a binary mixture can be challenging. IR or Raman spectra may be misleading because of either band overlapping by the fluorescence [15]. Furthermore, specific properties of each individual pigment present in the mixture, their heterogeneity (size of particles) as well as the chemical reactions between copper and oleoresinous media [16] makes data interpretation more complicated still. Some studies by Raman and IR spectrometry [17–20] Fibre-Optics Diffuse-Reflectance Spectroscopy FORS, Optical and Colorimetric Characterisation [21], X-Ray Fluorescence (XRF) [22], MidIR Fibre Optic Reflectance (MidIR-FORS) [23,24], Surface Enhanced Raman Spectroscopy (SERS) [25] and Chemometric Techniques [18,26] have been applied to solve the identification of a pigment in a mixture. Despite robust results obtained for some pigments, in the case of copper-based green pigments with the same colour and Cu-containing, precise identification is not possible using elemental analysis alone [27–29]. This analysis needs to be combined with other techniques to identify the chemical and molecular composition of these pigments.

The focus of the present study is therefore mixtures of green copper-containing pigments, present in the palettes of artists since Classical Antiquity, Egypt, Greece, Rome and Byzantium [5]. Of the green pigments available to said artists (green earth, viridian, emerald green...), the three pigments selected for this study (malachite, verdigris, and copper resinate) are those typically employed in the easel paintings of Alonso Cano (17th century) [30,31]. The goal is to evaluate the effectiveness of molecular spectroscopy techniques, μ RS and μ FTIR-ATR, to discriminate these binary mixtures, even when one of the components is in low proportion.

Furthermore, the study aims to establish the minimum percentage necessary of one of the Cu-containing pigments to be detected in the binary mixture. To that end, two sets of model samples were prepared with pure pigments and in three binary mixtures, in variable weight concentrations and exposure times within the controlled conditions of a climatic chamber. As a result, the study provides a precise reference library of the spectroscopic signature of each pigment in the specific mixtures (at multiple proportions and artificial ageing times), further aiding the interpretation of the spectra acquired from real painting analysis. The paint samples used were sampled from the green-coloured areas of easel paintings by Alonso Cano, a well-known artist of the Spanish Golden Age [32]. His artwork has been the focus of study by our Research Group over the last several years, financed by three National Projects (BHA2003–08671, HUM2006–09262, HAR-2010–19,411). The study was exemplified by the analysis of three historical paintings, *The Nativity*, *The Visitation*, and *The Assumption* (that are part of the iconographic program about the Life of the Virgin that Alonso Cano (Granada, Spain, 1601–1667) painted for the Main Chapel of the Granada cathedral (Spain). Alonso Cano, painter, sculptor, and architect is considered one of the most original and brilliant artists from the so-called Spanish Golden Age (17th century) and the founder of the school of Baroque painting in Granada (Spain) [32]. *The Nativity* represents the scene of the Virgin Mary's birth wherein Saint Joachim offers the Virgin Child to God and to heaven, while Saint Anne, in the background, rests on a bed with a large red canopy, the colour of blood and a symbol of Christ's humanity. *The Visitation* represents the visit of the Virgin Mary to her cousin Saint Elizabeth, upon learning from the archangel Saint Gabriel that she had conceived a son in her old age, despite being sterile and in the sixth month of her pregnancy. *The Assumption* represents the ascent of the Virgin Mary to heaven, propelled by a superior force, while the angels sustain the globe on which the figure of the Virgin is poised.

3. Materials and methods

3.1. Green pigments and binder medium

The green pigments selected for the study: malachite/10,300 (M), (basic copper carbonate); verdigris/44,450 (V), (copper(II)-acetate-1-hydrate); and copper resinate I/12,200 (CR), (copper (II)-acetate-1-hydrate 8–10%, colophony 60%, white spirit 30%); supplied by Kremer pigments (Germany). Refined linseed oil/73,300 supplied by Winsor & Newton (London, England) was employed with all pigments to manufacture the paints.

3.2. Model paint samples

Two sets of model samples were prepared using a white commercial canvas (40 40 × 40 mm) as the support (Fig. 1). The selected historical medium was refined linseed oil, supplied by Winsor & Newton (London, England) and was used in all samples (0.6 ml). The first set of samples was made up of the single green pigment (CR, M and V) mixed with the binder. The amount of linseed oil integrated in the model paint samples simulated the standard proportions in pigment mixtures, which must have an optimal consistency, not drip during application, and achieve a homogeneous layer. Due to pigment grain size, form, and composition, the oil absorbed by each pigment varies, but the optimal pigment/linseed oil (w/w) proportion required to obtain a viscous paint for each pigment studied was approximately 3:1 (1.5 g of pigment to 0.6 ml of linseed oil).

The second set of samples was prepared mixing two of the three green pigments in variable weights from 20% to 80% for each

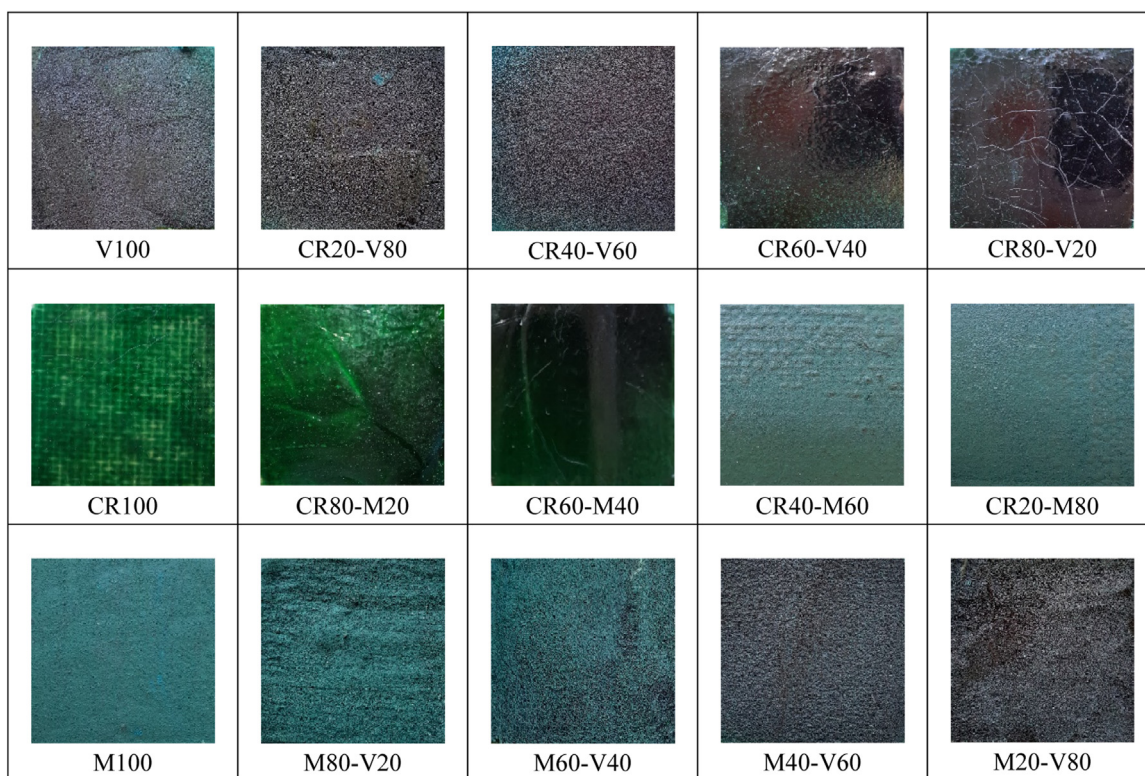


Fig. 1. Model sample sets.

Table 1

Three historical paintings, a) The Assumption, b) The Visitation, and c) The Nativity by Alonso Cano



component. These binary mixtures were then combined with linseed oil in the fixed proportion of 3:1 (w/w) of powdered pigments mixture to binder. All samples were carefully spread on painting canvas with a palette knife. Each layer was allowed to dry thoroughly before applying the subsequent one, allowed to dry freely without exposure to direct light and, after 1–2 weeks, was aged under controlled conditions in a climatic chamber (ISO 11,241:2004).

3.3. Case study: 17th century easel paintings by Alonso Cano

The study was exemplified by the analysis of three historical paintings, *The Nativity*, *The Visitation*, and *The Assumption* (Table 1), that are part of the iconographic program about the *Life of the Vir-*

gin that Alonso Cano (Granada, Spain, 1601–1667) painted for the Main Chapel of the Granada cathedral (Spain).

3.4. Cross sections

To analyse heterogeneous real paintings, cross-section preparation is required. To this end, a total of four micro-fragments were carefully sampled by the restorer from green areas of the three selected paintings with a scalpel and were subsequently embedded in Technovit resin, microtomed and polished with a Struer Tegrapol-15. Cross section images were obtained using an Olympus BX60 Microscope equipped with an LM Plan FI 20x/0.40 lens and a DP 70 12.5 Megapixel CCD Camera. Reflected light was used in all cases due to the thickness of the cross-sections.

Table 2
Raman wavelengths of unaged and aged model samples prepared mixing two of the three green pigments studied in variable weight from 20% to 80% per component.

MALACHITE + VERDIGRIS MALACHITE M100		M + V (80–20%)		M + V (60–40%)		M + V (40–60%)		M + V (20–80%)		VERDIGRIS V100	
t0	t144	t0	t144	t0	t144	t0	t144	t0	t144	t0	t144
2995vw											
2912vw	2935vw		2908vw	2917vw		2915vw					
2844vw	2848vw	2875vw		2861vw						2811vw	
1733vw	1723vw								1747vw	1770vw	
1626vw	1630vw	1645w		1627vw		1634vw		1652vw	1687w		
1491m	1484w	1497m	1486m	1500m	1489m	1497m	1490m				
1435vw	1433m	1446m	1450w	1453m	1448w	1448w		1437vw		1422vw	
1397vw	1401vw	1379m	1371w								
1364m	1358m	1371m	1360w	1373m	1362w	1371w	1364vw				
1290vw	1300w	1284w	1295w	1311w		1313w	1303vw		1298vw		
				1279vw	1279vw					1262vw	1258vw
				1104m		1105m		1117vw		1105sh	1103m
1092m	1085m	1087m	1085m	1072s	1089m	1065m	1085m	1092w	1086w		
1054m	1056m	1072s	1051m			1057m	1057m		1050vw		
			962w		950w	958m	969w	957m	939vw	945m	
		849w	880vw	879w	874w	880w	863w				877vw
715w	710w	727w	713w	726m	717w	730w	717w	717vw	726vw		
										686m	673m
			593w		599w	607w	587m	592m		587s	587m
529m	527m	522m	529m	542m		541m	533m				
508w	501w		505w	515m				496vw			
429s	427s	443s	428s	441s	430s	442s	430s	456w	436w		
407vw	402vw							404vw		401vw	405vw
349m	343m	361s	344m	360m		357w	346w				
						329w		321w	327w	318vw	322w
272m	262m	281s	264s	281m		279s	266s	303w	285m	287s	279s
COPPER RESINATE + VERDIGRIS											
COPPER RESINATE CR100		CR+V (80–20%)		CR+V (60–40%)		CR+V (40–60%)		CR+V (20–80%)		VERDIGRIS V100	
t0	t144	t0	t144	t0	t144	t0	t144	t0	t144	t0	t144
2930sh	2920sh	2936m	2930vw	2935m	2920m	2934vw		2938w			
2862sh	2859vw			2825w	2862m					2811vw	
1742vw		1745vw		1731vw	1725vw	1763vw				1770vw	
1650m	1640vw	1654m	1645vw	1649m							
1603vw	1598w	1619m	1622vw	1618m	1604m			1606w			
1445s	1438m	1451s	1433m	1450s	1442m	1448w	1426vw	1434m		1422vw	
1300m	1294w	1308m	1285w	1312m	1307m						
1255vw		1258w		1253vw						1262vw	1258vw
1193m		1206w	1206vw	1208w	1192vw	1186vw		1223vw			
						1106w			1113m	1105m	1103m
		1084m	1097vw	1075m	1079w		1087m				
		1019w		1028vw	1053m	1043vw	1031vw				
		935w	956vw	956m	935vw	959m		948s	959vw	945m	
		860w	886vw	851vw	842vw	836vw	853vw	846vw	880vw		877vw
710s	705m	714s	712m	716m	702m	699vw	702w				
		585vw	583vw	577w	588w	584s	604w	695m	690vw	686m	673m
452m	444sh	451w	458sh	443w	432vw		445w	580w	582s	587s	587m
403vw		404vw	407w	407vw	405vw		408vw	397vw	400w	401vw	405vw
	326vw	329w	328vw	327s	321w	321w	329w	311s	324vw	318vw	322w
284vw	285vw		286vw	284w		298s	279s	274vw	283s	287s	279s
COPPER RESINATE + MALACHITE											
COPPER RESINATE CR100		CR+M (80–20%)		CR+M (60–40%)		CR+M (40–60%)		CR+M (20–80%)		MALACHITEM100	
t0	t144	t0	t144	t0	t144	t0	t144	t0	t144	t0	t144
2930sh	2920sh	2927m	2926vw	2923vw	2922vw	2910vw				2995vw	
2862sh	2859vw	2863m	2843vw	2868vw						2912vw	2935vw
1742vw										2844vw	2848vw
1650m	1640w	1648m	1646w	1648w		1640w		1659w		1733vw	1723vw
										1626vw	1630vw
1603w	1598w	1605m	1603w	1611w	1597m		1605vw		1595vw		
					1485w	1497w	1485m	1485m	1488m	1491m	1484w
1445s	1438m	1438s	1436m	1437m	1438m	1450w	1437m	1439m	1432vw	1435vw	1433m
		1381vw							1404w	1397vw	1401vw
						1372w		1365w	1358w	1364m	1358m
1300m	1294w	1303m	1292w	1297m	1298m	1313w	1304w	1301w	1300w	1290vw	1300w
1255vw	–	1254w		1240vw	1242vw	1242w					
1193m	–	1194m	1191vw	1198w							
		1099w		1081m	1081m	1104m		1090s	1090m	1092m	1085m

(continued on next page)

Table 2 (continued)

MALACHITE + VERDIGRIS MALACHITE M100		M + V (80–20%)		M + V (60–40%)		M + V (40–60%)		M + V (20–80%)		VERDIGRIS V100	
		1062m	1040w	1067m	1050m		1074m	1057s	1060m	1054m	1056m
		966vw	963vw								
		881sh	879vw	883w	883w		867vw	868w	862vw		
710s	705m	705s	703m	703m	698m	707m	702vw	718w	718vw	715w	710w
		596vw	602vw	603vw	613w	594vw		596vw			
				508w		517w		510w	505w	508w	501w
							528w	534m	533w	529m	527m
452m	444sh	456m	431m	429m	426m	443s	426s	430s	427m	429s	427s
403vw	–									407vw	402vw
–	326vw	321w	320w	321vw	328vw	359m	347w	351m	349m	349m	343m
284w	285w	290w	311w	271w	279m	279m	263m	269s	272m	272m	262m

Aged linseed oil Raman bands: 3009 w, 2900vw, 2851 w, 1740 w, 1654s, 1436s, 1396vw, 1298 m, 1263s, 1066 m, 1015 w, 967 w, 866 m, 718 w, 402vw, 319vw y 289 w cm⁻¹.

s = strong, m = medium, w = weak, v = very, sh = shoulder, br = broad.

3.5. Variable pressure scanning electron microscope (VP-SEM)

Energy dispersive X-ray spectroscopy (EDX) was used to determine the elemental composition of individual particles using scanning electron microscopy (SEM). Cross sections were examined with a Variable Pressure Scanning Electron Microscope (VP-SEM) ZeissSupra 40Vp. Maximum resolution: 1.3 nm; acceleration voltage: 0.2–30 kV; software: SmartSEM. An Aztec 2.2 EDX system equipped with an XMAX 50 mm² silicon drift detector was also used. Energy dispersive X-ray spectrometry imaging (EDX mapping) was used also to provide chemical maps of the components of all areas of the cross-section samples.

3.6. Attenuated total reflectance - Fourier transform infrared spectroscopy (μ FTIR-ATR)

Model paint samples were analysed by a JASCO 6200 spectrometer coupled with a JASCO IRT7100 microscope which uses attenuated total reflection with a diamond ATR crystal. The measurements were run in the 600–4000 cm⁻¹ range with 2 cm⁻¹ resolution and 300 scans. The data was processed using Spectra Manager II software.

Each sample was characterised with five genuine replicates. Thus, five different points were measured per sample, under the same experimental conditions. Figure S1 in the Supplementary Information (SI) provides an example of the five repeated IR spectra performed on selected sample ACC2.11 and V100 model samples. In addition, in Figure S1, also five repeated Raman spectra were included (ACC2.11 and M40-V60 model sample). Given the similarity of the spectra, any of them served to establish the wavelengths in the corresponding tables. The absorption bands were compared to spectroscopic signatures of pure pigments performed in the present study and checked with reference data in the literature [28,33] including the Infrared and Raman Users Group (IRUG) database [34].

3.7. Micro-Raman spectroscopy (μ RS)

Raman spectra of the model paint samples were obtained with a dispersive μ Raman spectrometer JASCO NRS5100. A 785 nm red diode laser of 500 mW (Torsana Starbbright) was employed, in addition to being cooled by a Peltier-cooled CCD detector on an Olympus confocal microscope (x5, x20, and x100 lenses). The 520.7 cm⁻¹ silicon standard peak was used for calibration. A digital camera attached to the microscope allowed the visual examination and the selection of sampling areas. To avoid thermal degradation, only a few milliwatts of laser power was used. Spectra Manager II software was used for system control, data acquisition and analysis. A

slight smoothing process was performed to reduce noise. The defined spectral range was between 200 and 3500 cm⁻¹, with a resolution of 1 cm⁻¹. Spectral measurements were carried out with exposure times of 25 s and five accumulations. In addition, an attenuator OD1.3 was used to avoid degradation. Each sample was characterized with five replicates of an μ RS spectrum. The evaluation and interpretation of the Raman spectra from the real painting was compared with reference library data of the spectroscopic signature of pure pigments, available in reference spectra literature [10,28,33,35,36] including the IRUG database [34].

3.8. Climatic chamber

The reference samples were aged artificially in a Solarbox 3000eRH climatic chamber by exposure to sunlight using a 2500 w Xenon lamp. Radiation was controlled by a soda-lime glass UV filter to simulate outdoor exposure, and temperature monitored with a BST (Black Standard Thermometer). The experimental conditions, according to ISO 11,241:2004 were 80 °C, 65% relative humidity and 550 W/m² irradiances, with ageing intervals of 0 h, 24 h, 48 h, 72 h and 144 h. After each exposure time, μ FTIR-ATR and μ RS were applied jointly to identify the green pigments (malachite, copper resinate or verdigris) in both single and binary mixtures.

4. Results and discussion

The first data discussed is that acquired using μ FTIR-ATR and μ RS on the single and binary model samples after accelerated ageing with UV irradiation for durations of 0 h, 24 h, 48 h, 72 h and 144 h. Subsequently the Raman and IR measurements were tested on cross-sections of micro-samples sampled from selected green areas of Alonso Cano's historical masterpieces. The results are contrasted with the elemental composition EDX microanalyses and the morphological observations of both optical and electron microscopy.

4.1. Model paintings

4.1.1. Single model samples

Raman and IR spectrum of each pure pigment was analysed and both band wavenumbers (cm⁻¹) and relative intensities (vw, w, m, s, sh, br) were collected in the first and last columns of Tables 2 and 3, respectively. (Figure S2, from Supplementary Information, include Raman and IR spectra of each single pigment and binary model samples in variable weight concentrations and various ageing time). To simplify the tables, only the wavelengths of the peaks found on the spectra at 0 h and 144 h of ageing time are listed. Since the pigment or pigments were mixed with linseed oil

Table 3

ATR wavelengths of unaged and aged model samples prepared mixing two of the three green pigments studied in variable weight from 20% to 80% per component.

MALACHITE + VERDIGRIS											
MALACHITE M100		M + V (80–20%)		M + V (60–40%)		M + V (40–60%)		M + V (20–80%)		VERDIGRIS V100	
t0	t144	t0	t144	t0	t144	t0	t144	t0	t144	t0	t144
3397m	3397w	3483w		3470vw		3466vw		3458w		3467m	3400–3500br
3303m	3298w	3396m	3396w	3397m	3396w	3397m	3396ve	3369w			
		3308m	3301vw	3309m	3310w	3369w	3302vw	3369w		3367sh	3366m
				3271vw		3269w		3271w		3268m	3367sh
						2984vw		2985vw		2987w	2988vw
2925m	2925w	2925m	2921w	2924m	2925w	2927w	2925w	2927w	2928w	2936w	2926w
2855m	2852w	2853m	2848vw	2853m	2854w	2854w	2854w	2855w	2855w	2854w	2854w
1736m	1734m	1735m	1743m	1735m	1735m	1739w	1737w	1740w	1737w	1734w	1734w
		1595w	1596w	1595w	1522m	1594s	1543m	1595s	1545s	1595s	1540s
1485m	1485m	1485m	1489m	1488m	1496w	1507vw				1442w	
				1435vw		1436vw		1440w		1442w	
		1411vw	1407vw	1413vw	1409vw	1417s	1390s	1417s	1411s	1417s	1409s
1372s	1375s	1377s	1375m	1379s	1384s	1351vw	1351vw	1354vw	1354vw		
1237vw	1237vw			1242vw		1240vw		1249vw			
1163w	1163w	1165m	1160m	1165w	1159w	1165w	1166vw	1164w	1162vw	1167vw	1168vw
1096m	1095w	1094m	1094w	1094m	1095m	1095w	1095w	1096m	1095w		
1033s	1038s	1037s	1038m	1033s	1041s	1047m	1043m	1047m	1046m	1048m	1048vw
			1038m	1033s		1032m		1032m	1025m	1032w	1022w
867m	862m	865s	864m	866m	866m	870w	869w	871w	873w		
815s	815s	816s	816m	816s	817m	818m	818m	819w	819w		
771w	771w	772w		773w	775w	773vw	776vw	769vw			
747s	747s	746m	747w	746m	748m	747vw	749w	744vw	750vw		
		712w	711w	710w		714vw					
			687w	686s	679w	686s	681m	685s	676m	686s	673m
		627w	626vw	625w	616vw	625m	618vw	625s	625vw	626m	625vw
565m	565m	568s	568m	569s	569w	559w	567w	553vw	578vw		
523w	523w	521m	520	521w	517vw	522vw	516vw	520vw	511vw	520vw	525vw
COPPER RESINATE + VERDIGRIS											
COPPER RESINATE CR100		CR+V (80–20%)		CR+V (60–40%)		CR+V (40–60%)		CR+V (20–80%)		VERDIGRIS V100	
t0	t144	t0	t144	t0	t144	t0	t144	t0	t144	t0	t144
3429sh	3396sh	3397sh	3376sh	3448sh	3464w	3465w	3452vw	3465w	3452w	3467m	3400–3500br
				3364w	3367w	3363w	3367vw	3367w	3367w	3366m	3367sh
				3260vw	3269w	3268w	3271vw	3268w	3269w	3268m	
					2984vw	2984vw	2978vw	2984w	2978vw	2987w	2988vw
2927s	2931m	2925s	2930m	2926s	2928w	2936vw	2929w	2932w	2928w	2936w	2926w
2856m	2870vw	2856m	2871vw	2855m	2849w	2856vw	2852w	2855w	2855w	2854w	2854w
					1743w	1734vw	1735w	1735w	1743w	1734w	1734w
1694s	1712s	1696s	1714s	1707s	1710w	1710vw	1718vw				
1610m	1600m	1607m	1600m	1607m	1599s	1594s	1582s	1595s	1585s	1595s	1567s
1460m	1456vw	1457m									
				1443w	1440vw	1442vw	1442vw	1442vw	1433vw	1442w	
				1409vw	1403vw	1415s	1417s	1409s	1417m	1415s	1417s
				1386w	1380vw	1386w	1353w	1354m	1350w	1354m	1409s
1382m	1382w	1386w	1380vw	1386w	1353w	1354m	1350w	1354m	1353m		
1239m	1227vw	1221vw	1237m	1237m	1249vw	1247vw	1247vw	1255w	1242vw		
1170m	1162m	1170m	1159m	1166m	1157w	1165vw	1166w	1165w	1169w	1167vw	1168vw
			1051w	1049m	1048w	1050m	1048w	1048w	1049m		
		1036w	1047w	1032w	1033m	1032m	1034vw	1032m	1033m	1048m	1048w
										1032w	1022w
		696w	675w	686m	686s	686s	688s	686s	686s	686s	673m
				624w	625m	625s	622m	625s	625m	626m	625vw
				527vw		514w	518w	525w		520vw	525vw
COPPER RESINATE + MALACHITE											
COPPER RESINATE CR100		CR+M (80–20%)		CR+M (60–40%)		CR+M (40–60%)		CR+M (20–80%)		MALACHITE M100	
t0	t144	t0	t144	t0	t144	t0	t144	t0	t144	t0	t144
3429sh	3396sh	3400sh	3397sh	3397vw	3397sh	3397w	3399w	3397w	3389w	3397m	3397w
				3316vw		3309w	3309w	3307w	3301w	3303m	3298w
2927s	2931m	2925s	2932m	2926m	2934m	2925m	2927w	2925m	2926w	2925m	2925w
2856m	2870sh	2855m	2867vw	2855w	2867vw	2854w	2857w	2854w	2860w	2855m	2852w
						1732m	1730m	1735m	1735m	1736m	1734m
1694s	1712s	1695s	1710s	1710s	1713s	1718m					
1610m	1600m	1607m	1606m	1606m	1608m	1608w	1618w	1614w	1618w		
1460m	1456sh	1458m	1453vw	1457w		1489m	1488m	1486m	1489m	1485m	1485m
1382m	1382w	1385m	1380m	1383m	1380m	1378s	1380s	1377s	1375s	1372s	1375s
1239m	1227sh	1240m	1231vw	1236w	1237vw	1241w	1237vw	1242w	1234vw	1237vw	1237vw
1170m	1162m	1169m	1161m	1165m	1159m	1166w	1159w	1165w	1162w	1163w	1163w
		1104w	1095vw	1095w	1094w	1094m	1095w	1094m	1094w	1096m	1095w
		1037w	1044vw	1042m	1042w	1038s	1041s	1039s	1037s	1033s	1038s
		876vw		870w	874w	864m	870m	865s	862m	867m	862m

(continued on next page)

Table 3 (continued)

MALACHITE + VERDIGRIS		MALACHITE M100		M + V (80–20%)		M + V (60–40%)		M + V (40–60%)		M + V (20–80%)		VERDIGRIS V100	
		820w	819vw	818m	818m	816s	818s	816s	815s	815s	815s		
				772vw	773vw	773w	773vw	772w	774w	771w	771w		
			748vw	747vw	747vw	746w	748m	746m	747m	747s	747s		
		710w			707vw	710w	711w	710w	710w	712w	711w		
		567vw	566vw	569w	570w	569m	571m	569m	568m	565m	565m		
			514w	521vw	519vw	521vw	523vw	521w	519w	523w	523w		

Aged linseed oil IR bands: 2996 w, 2919s, 2850 m, 1737 m, 1710vw, 1464 w, 1375 w, 1237 w, 1168 m, 726 w cm⁻¹.

s = strong, m = medium, w = weak, v = very, sh = shoulder, br = broad.

in the model samples, only the wavelengths specifically attributed to the absorption of the pigment (not the linseed oil) appear in bold in the tables. These indicated bands will be used for reference purposes since they remain in the spectrum after ageing or mixing. The performance of the linseed oil bands was cross referenced with the IRUG database [34] and listed at the bottom of the above-mentioned tables. The IR and Raman spectra of the pure pigments were in line with (or at least the main bands match) those reported in the literature [10,28,33,35,36]. It should be noted that the spectrum of the aged verdigris shows slightly shifted wavelengths, some bands even disappearing altogether, compared to the unaged verdigris. This is attributed to the chemical change that this pigment undergoes when ageing in the presence of copper salts of fatty acids, turning the verdigris into copper resinate [28].

Since our intention is the application of the results to the study of historical paintings, the use of 532 nm excitation was avoided because of the fluorescence that would be generated. Nevertheless, despite the use of a 785 nm laser, the resulting Raman spectrum in some binary samples shows too much fluorescence with poorly resolved peaks, the wavelengths of which are listed in the first column of Table 3. On the other hand, the IR spectra is more revealing of the pigments' and mixtures' changes with ageing. Fig. 2 shows the comparison of the IR spectrum of every unaged (0 h) and aged (144 h) pigment, allowing conclusions to be made on the stability of each pure pigment studied after artificial ageing of up to 144 h. Tables 2 and 3 collect the main Raman and IR wavelengths results, respectively.

Regarding the IR spectra of unaged and aged malachite (Fig. 2-a), in agreement with the literature [37], significant differences in the frequency of its bands were not detected, suggesting that pure malachite is stable during ageing. Visible IR bands correspond to typical features of the two hydroxyl stretching bands at 3397 and 3298 cm⁻¹, from the carbonate group at 1485, 1375, 1095, 1038, 862, 815, 771 and 747 cm⁻¹ and Cu-O at 565 and 523 cm⁻¹, the wavelengths of which match unaged malachite. The comparison of the main Raman bands of unaged malachite (1491, 1364, 1092, 1054, 529, 429, 349 and 272 cm⁻¹) and aged (1484, 1358, 1085, 1056, 527, 427, 343 and 262 cm⁻¹) also confirm its stability. Nevertheless, the less or slower reactivity of malachite in comparison with verdigris was reported [16,37]. No Raman bands were observed at the 3000–4000 cm⁻¹ region of aged verdigris [38]. The IR bands of the unaged verdigris at 3467 and 3266 cm⁻¹ become a broad band in the case of the aged verdigris at 3400–3500 cm⁻¹ with a shoulder at 3367 cm⁻¹, due to the OH stretching mode of the water molecule associated to the acetate ion spectra of unaged verdigris (Cu(CH₃COO)₂·H₂O) (Fig. 2-b). Two bands of unaged verdigris at 1442 and 626 cm⁻¹ disappear after 48 h of UV treatment. The more intense and stable IR wavelengths of aged verdigris are shown in bold in the last column of Table 3. The weak IR band found at 1734 cm⁻¹ in the model sample of verdigris (also malachite) could be attributed to carboxyl group of linseed oil, as well as the 2988, 2926 and 2854 cm⁻¹ weak bands to the CH bond also characteristic of the binder, so they were not included in

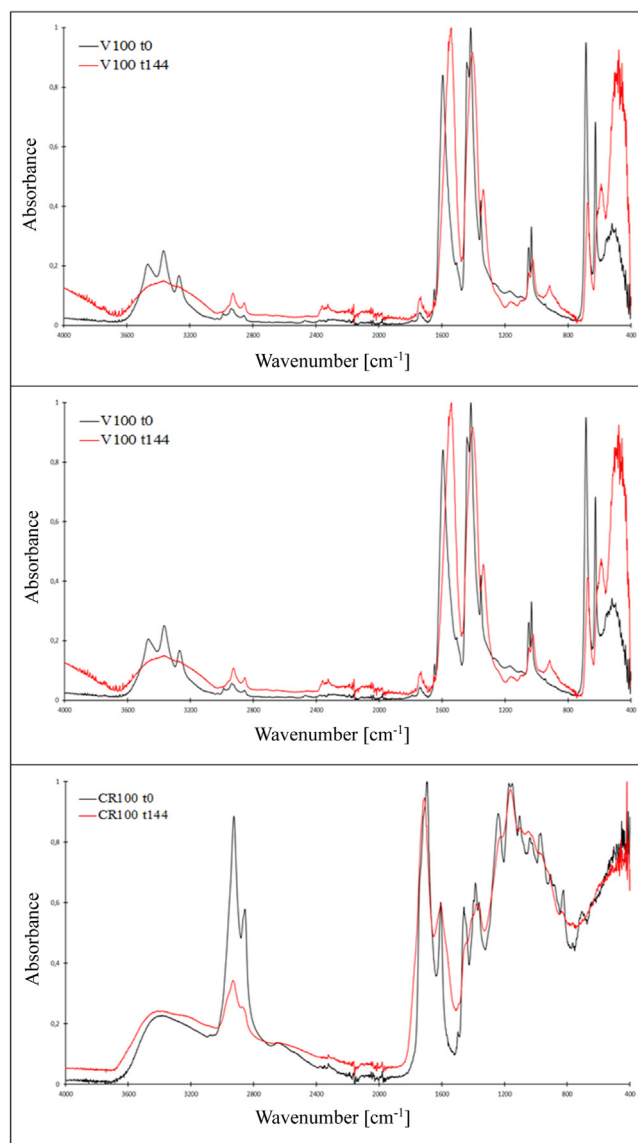


Fig. 2. Comparison of the IR spectra of every unaged (0 h) and aged (144 h) pure pigments, a) malachite (M100), b) verdigris (V100) and c) copper resinate (CR100).

bold in the table. Ageing of copper resinate represents an increase in the fluorescence signal that overlaps many of the bands of the Raman spectrum or appear at lower intensity and shifted slightly from unaged CR. Weak peaks were observed on the IR spectrum from aliphatic chains of conifer resins (at 2931 and 2870 cm⁻¹, at 1600 cm⁻¹ and 1712 cm⁻¹) to ionized carboxyl and carbonyl groups, compatible with the copper salts of resin acids, that could be key to its differentiation to the verdigris pigment (Fig. 2-c).

4.1.2. Binary model sample

Tables 2 and 3 collected Raman and IR wavelengths of unaged and aged pure pigments and their binary mixtures. Regarding aged malachite, the Raman wavelengths at 1056 and 427 cm^{-1} remain in the spectrum of the mixture with CR or V, even when malachite is only 20% present (CR80-M20 and M20-V80 model samples). Additionally, the peaks at 1484 and 1085 cm^{-1} , characteristic of the Raman spectrum of malachite, is consistent with the CR+M mixture up to 40% of M. However, the only verdigris Raman band at 587 cm^{-1} that remains visible in the mixtures (CR+M and M+V) up to 50% is not sufficient to distinguish its presence. Copper resinate in the mixtures with verdigris or malachite behave similarly, requiring a percentage higher than 60% for its identification (see the peaks at 1598, 1438 and 705 cm^{-1} in Table 2). It is noteworthy that the Raman band at 1438 cm^{-1} of CR can be confused with the weak band of M at 1433 cm^{-1} of the CR+M mixture.

In the case of IR bands of malachite, its primary identifying wavelengths were present in the mixture with both V or CR, even for small percentages of M (M20-V80 and CR80-M20 mixtures). Nevertheless, discriminating the presence of verdigris in these mixes was more complex. Fig. 3 provides the $\mu\text{FTIR-ATR}$ spectra of the 40:60 binary mixture and the corresponding pure pigments. Fig. 3-a shows the IR spectrum of the mixture of verdigris and malachite (M40-V60) as well as each pure pigment M100 and V100. Fig. 3-b shows the IR spectrum of the mixture CR40-M60 and each pure pigment CR100 and M100. Fig. 3-c shows the IR spectrum of mixture CR40-V60 and each pure pigment CR100 and V100. The selected spectra correspond to the samples aged for 144 h. The indicated bands on the spectrum of the mixture (black line) are those that matched one pure pigment or another and the corresponding wavelengths are included in each box. The spectrum of M40-V60 mixture (Fig. 3-a) retained visible bands attributable to malachite (3397, 3303, 2926, 2855, 1390, 1164, 1095, 1043, 869, 818, 749 and 567 cm^{-1}) but only two typical peaks of verdigris remained (1544 and 681 cm^{-1}). Similarly, with the CR40-M60 sample (Fig. 3-b), the typical malachite bands remained. Nevertheless, CR40-V60 (Fig. 3-c) shows characteristic bands of both copper resinate (2929, 2852, 1718, 1582, 1350 and 1166 cm^{-1}) and verdigris (1582, 1409, 1166, 1050 and 688 cm^{-1}), making their discrimination in the mix difficult. It is known that identification of verdigris and its differentiation from copper resinate is a challenging task due to the reaction of verdigris in contact with copper salts of fatty acids [28], among other causes. According to the literature, the presence of Raman lines in the 1600–1700 cm^{-1} region due to the C=C stretching seems likely to be compatible with the copper salts of resin acids, facilitating its discrimination in a verdigris mixture [10]. In the present study, a weak Raman band at 1598 cm^{-1} of copper resinate was observed, which remains visible in the mixtures up to 60% presence with verdigris. In the IR spectrum, wavelength at 1600 cm^{-1} to ionized carboxyl group and at 1712 cm^{-1} in aged copper resinate assigned to carbonyl group stretching are related to the abietic acid and abietane skeleton acids, such as 7-oxo dehydroabietic, observed in the mixtures at even 40% of CR (1582 and 1718 cm^{-1} in CR40-V60 sample). The IR band at 1382 cm^{-1} may prove useful, associated with symmetric stretching of the COO- group of copper abietate of coniferous resins, present in the CR+V and CR+M mixture spectrums, even at only 20% of CR.

4.2. Historical paintings

Four micro-samples, sampled from green pigmented areas of the three Baroque masterpieces The Nativity, The Visitation, and The Assumption by Alonso Cano, were embedded in resin and polished to obtain a cross-section as described in the experimental

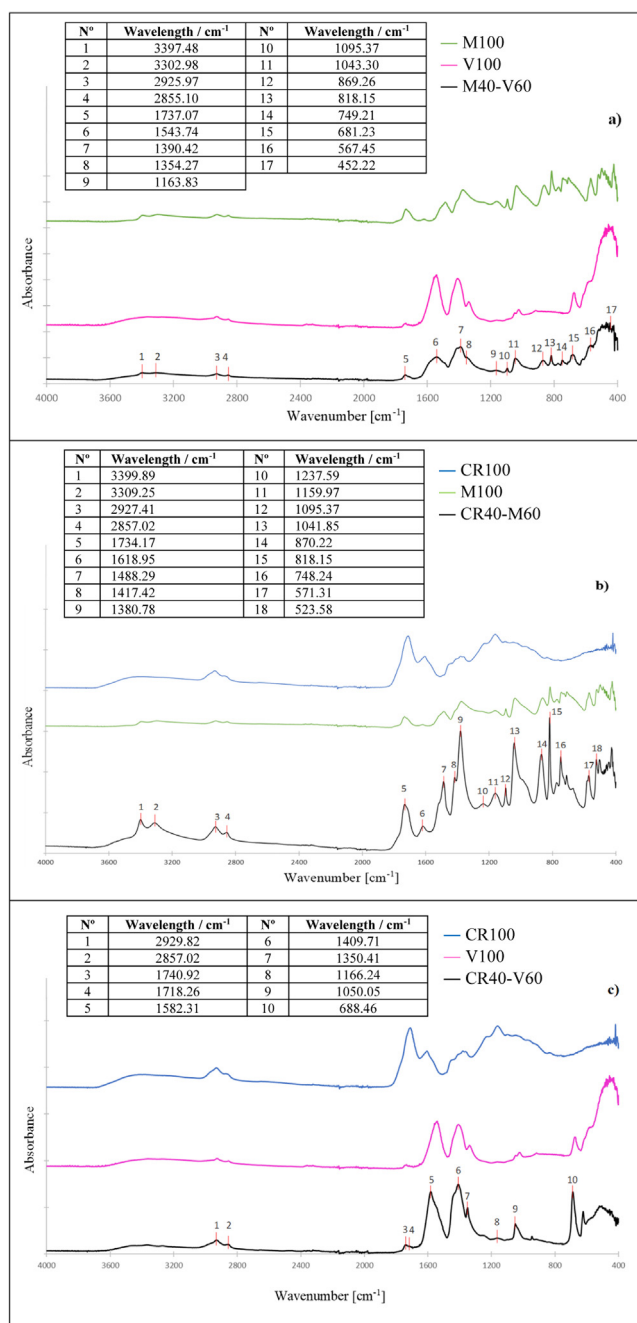


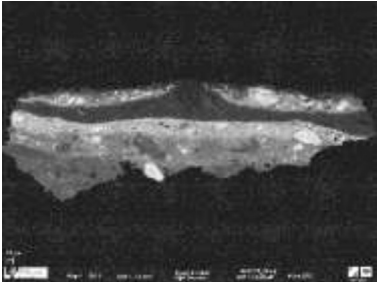
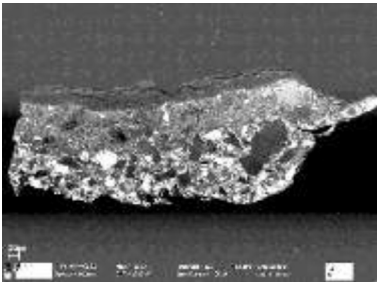
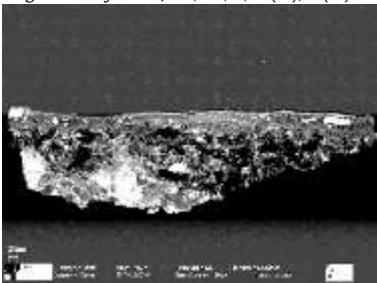
Fig. 3. IR spectra of three binary sample at 40:60 proportion and their main wavelengths together the corresponding IR spectra of pure pigments what makes up each mix: a) M + V, b) CR+M and c) CR+V.

section. Conventional optical microscopy (OM) and scanning electron microscopy (SEM) were used for preliminary examinations, showing the light-optical micrograph and backscattered electron (BE) image in Table 4.

The metallic cations present by qualitative X-ray microanalysis (EDX) were collected in the last one, checking Cu in the green pictorial layer of all analysed cross-sections. It should be noted that the EDX results from The Visitation were previously published by our Research Group [30] while those from The Nativity and The Assumption were carried out in the current study. EDX mapping found a majority of copper present in the pictorial layer, but no other differences in elemental composition. Fig. 4 for selected ACC7.9 and ACC5.3 samples provides information on the distribu-


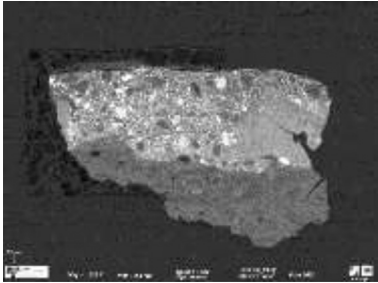
Table 4

Pigment samples from three Alonso Cano paintings. Sample descriptions. Nomenclature, sample sources, OM (Optical Microscopy) and SEM (Scanning Electron Microscopy) images of cross-sections and chemical elements found with EDX microanalysis (Energy Dispersive X-Ray Spectroscopy); (tr): trace elements; in bold: major elements. [a] Previous result analysis by our Research Group [30].

Painting	OM images of cross-section/green location/ sample nomenclature	SEM images of cross-section/EDX microanalysis (elements)
The Nativity	ACC2.11 sample Midwife's clothes	 5: glaze: Cu, Pb, Ca 4: pictorial layer 2: Cu, Ca 3: pictorial layer 1: Co, Si, Pb 2: ground layer: Fe, O, Si, Al, Na, Mn, Pb 1: ground layer: Fe, O, Si, Al, Mg, Na, Ca, K, Pb
The Visitation[a]	ACC5.3 sample St Elizabeth's green tunic	 3: glaze: Cu 2: pictorial layer: Si, Co, Cu, Pb 1: ground layer: Fe, Pb, Ca, S, Al(tr), Si(tr)
	ACC5.13 sample Green landscape – leaves	 3: pictorial layer-: Pb, Cu, K(tr) 2: pictorial layer-: Pb, Si, Co, K(tr), Al(tr) 1: ground layer: Fe, Pb, Ca, S, Al(tr), Si(tr)

(continued on next page)

Table 4 (continued)

Painting	OM images of cross-section/green location/ sample nomenclature	SEM images of cross-section/EDX microanalysis (elements)
The Assumption	ACC. 7.9 sample Angel wings 	 3: glaze: barniz 2: pictorial layer: Pb, Cu 1: ground layer: Fe, S Ca, Pb, Si, Al, P, Mn

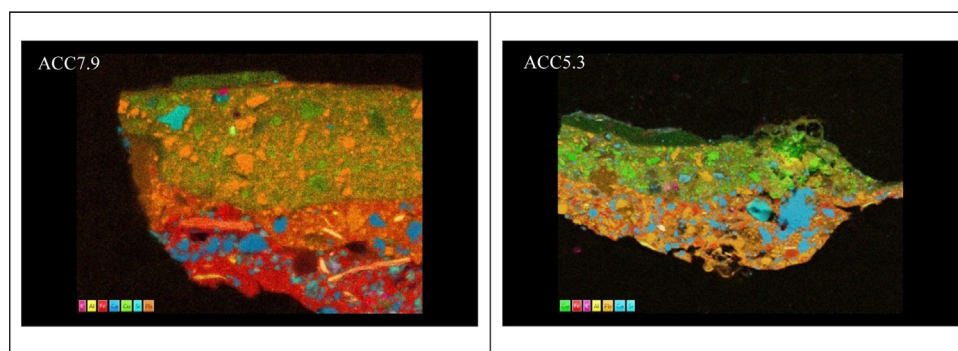


Fig. 4. EDX mapping for ACC7.9 and ACC5.3 samples.

tion of some elements within the painting cross-sections. Fig. 5 shows one of the five IR spectra performed on the green pictorial layer of ACC2.11, ACC5.3, ACC5.13 and ACC7.9 cross-sections. As expected, Raman spectra of real samples present high fluorescence and weak bands and does not contribute relevant information. As such, this information was not included.

The IR spectrum of the ACC2.11 sample display a broad weak band in the 3300–3500 cm^{-1} range, which also appears in hydrated acetates such as verdigris. There are no specific OH bands reported for the model sample of malachite at 3397 and 3298 cm^{-1} . The small band at 3532 cm^{-1} does not seem attributable to the green pigment but rather to characteristic bands due to OH stretching mode related to alumino-silicate groups. The five spectra performed along the green pictorial layer of the copper resinate model samples show a high intensity of stretching vibrational bands of the methyl group (2917 and 2850 cm^{-1}). The CH₂ bands may correspond to either the linseed oil medium or the hydrocarbon skeleton of the resin [39]. Fig. 6 shows the IR spectra of the ACC2.11 sample, along with those of the linseed oil and copper resinate, both aged, in the O–H and C–H stretching band range.

The matches found for the main wavenumbers selected from verdigris (1403 and 680 cm^{-1}), and the media-intensity band at 1584 cm^{-1} , are related to the antisymmetric stretching of the COO⁻ group [40], and which, based on the results of SEM-EDX (Table 2), allows us to suggest copper carboxylates (from copper resinate) present in the ACC2.11. According to the literature [10], it's difficult to distinguish V from CR in a real sample. The absence of Raman lines at 1598 and 1640 cm^{-1} in the ACC2.11 sample, as well as highlights on the model sample of copper resinate, indicate that CR was not present. Nevertheless, these weak Raman bands from CR are far from a useful diagnostic indicator for paintings as they will progressively disappear as the percentage of

verdigris in the mixture increases. Since all the Raman spectra performed from the green pictorial layer present high fluorescence, two weak bands at 1438 and 1299 cm^{-1} , typical of CR, support the microscopic observations. In addition, both wavelengths (in bold in Table 3) remain visible in the CR60-V40 spectrum. The IR spectra performed show a low-intensity peak at 1163 cm^{-1} wavelength (C–O stretch) that correlate with resin acid of the copper resinate model sample rather than the epoxy resin of the cross-section. The band at 1710 cm^{-1} due to C C = O group from abietane skeleton acids, and at 1403 cm^{-1} , associated with symmetric stretching of COO⁻ group [40], support the presence of coniferous resins. Finally, the high-intensity band at 680 cm^{-1} in ACC2.11 under study is assigned to the CH₂ rocking vibrations [41].

It was not possible to acquire Raman spectra in multiple micro areas in the green pictorial layer of The Visitation (sampled from Elizabeth's tunic and the leaves in the landscape), ACC5.3 and ACC5.13 samples, due to the high fluorescence observed. Nevertheless, the analysis of a small particle from the green pictorial layer of the ACC5.3 sample presented characteristic bands of the malachite pigment (1484, 1435, 1082, 1059, 713, 524, 426, 345 and 265 cm^{-1}). The characteristic Raman band of CR (pure) at 705 cm^{-1} (shown in bold in Table 3) is observable (although very weak) in three of the 7 replicates performed (at 702, 713 and 705 cm^{-1} , respectively) of ACC5.13 sample. The $\mu\text{FTIR-ATR}$ performed on The Visitation indicates a mixture of Cu-containing pigments. ACC5.3 sample shows a broad weak band in the 3300–3500 cm^{-1} , while ACC5.13 show two hydroxyl stretching bands at 3373 and 3253 cm^{-1} , both matching malachite. Other typical bands from malachite were observed (1095, 1047, 872 and 748 cm^{-1}). The symmetric and antisymmetric C–H stretching vibrations of methyl and methylene groups appear in both green layers around 2850 and 2980 cm^{-1} , observed in the copper resinate and linseed oil

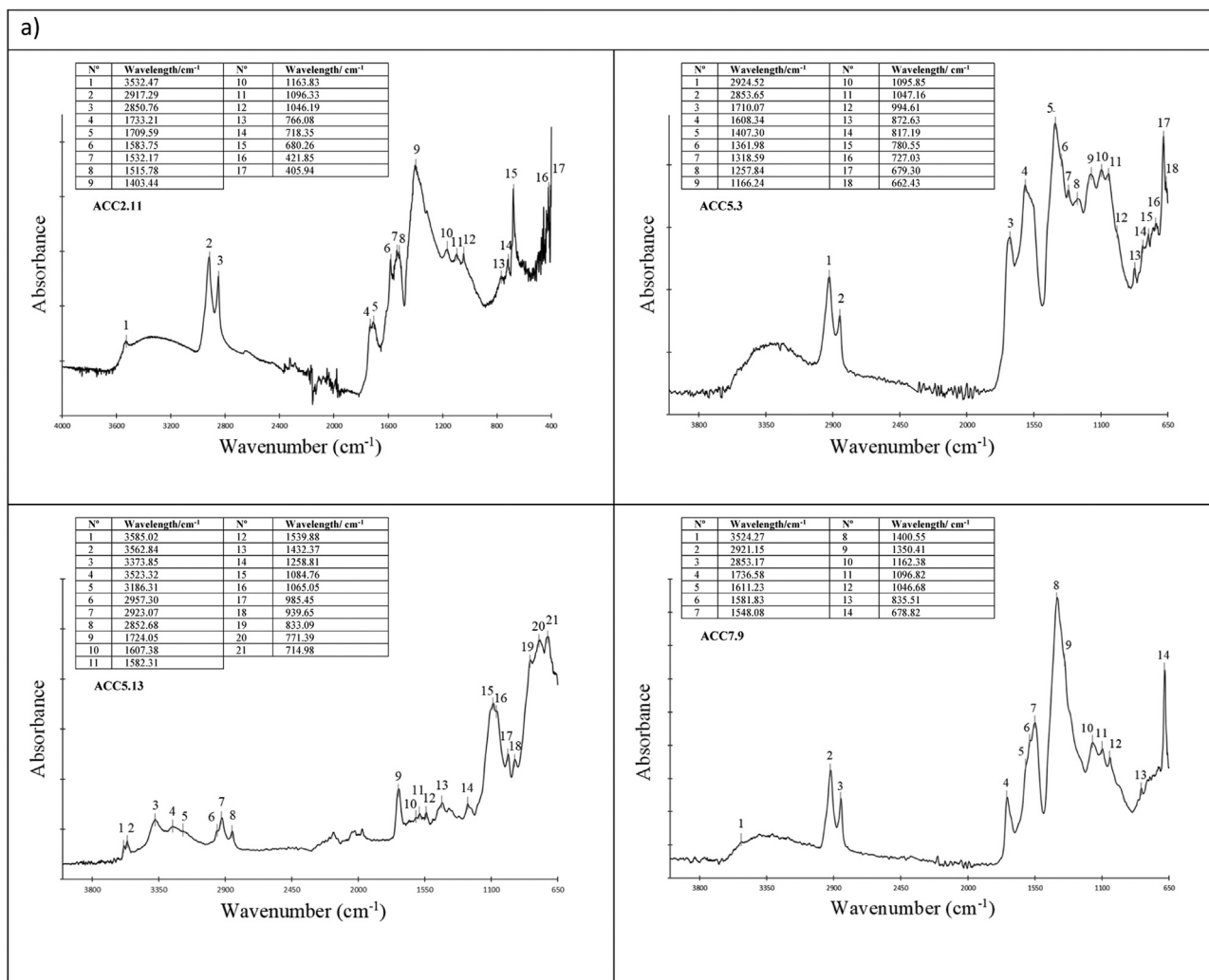


Fig. 5. IR spectrum a) Historical paintings: ACC2.11 sample (The Nativity); ACC5.3 sample (The Visitation); ACC5.13 sample (The Visitation) and ACC7.9 sample (The Assumption) and b) Single Model Samples: M100, V100 and CR100.

medium. Typical wavenumbers of verdigris and copper resinate are observed around 1400 and 680 cm^{-1} , and high-intensity bands at both 1608 cm^{-1} from the COO– group and at 1710 cm^{-1} (in the green landscape leaves) indicate a carbonyl group of acid resins from copper resinate. The peak at 1163 cm^{-1} matches resin acid.

An intense Raman band stands out in the spectrum of the pictorial layer from the ACC7.9 sample at 1048 cm^{-1} from lead white as well as typical wavelengths of malachite (1437, 1406, 1352 and 1298 cm^{-1}) supported by peaks at 1087, 1069 in others analysed micro areas. The IR spectrum of the ACC7.9 sample also showed a weak and broad band in the 3300–3500 cm^{-1} range, attributable to hydrated salts and olefinic C–H stretching absorption at 2921 and 2853 cm^{-1} of the resin Pinus or a linseed oil medium. A strong band at 1400 cm^{-1} stands out in the spectrum attributable to lead carbonate hydroxide (lead white), that could overlap verdigris and copper resinate peaks. Some wavenumbers from the model samples of verdigris (1540, 1400, and 687 cm^{-1}) and malachite (1736, 1096, 1046 cm^{-1}) that appear in the IR spectrum are bands that remain when both pigments are mixed.

5. Conclusions

The first step of this study consists of identifying spectroscopic marker bands (IR and Raman) characteristic of selected green pig-

ments mixed with linseed oil that remain after ageing under UV radiation up to 144 h. Next, the binary mixtures of the selected green pigments (at 20%, 60% and 80% proportions) were studied to evaluate the minimum quantities of a pigment necessary in a mixture to change its individual spectra fingerprint. This achievement provides easy-to-interpret data for professionals in conservation of Cultural Heritage. The specific spectroscopic library created was successfully used for reference purposes on three masterpieces of an outstanding artist from the Spanish Golden Age. With this first study it can be concluded that molecular analysis of mixtures of green pigments from historical paintings successfully identified them as copper based, using μRS and $\mu\text{FTIR-ATR}$, and could further discriminate the presence of malachite by its characteristic bands that remain visible over ageing in the spectrum, even when one of the components was mixed at low proportions. Therefore, malachite was identified as the main component of the paint layer of the ACC7.9 sample, mixed with lead white to lighten the green colour. The pigment seemed to be mixed with verdigris, the addition of which may not have been intentional, but rather present as dirt particles because of this pigment's prevalence in Alonso Cano's palette. In the green pigmented area of The Nativity (ACC2.11 sample) the main pigment was copper resinate, although verdigris could not be ruled out from the mix in some areas. No malachite was observed. The green from St Elizabeth's

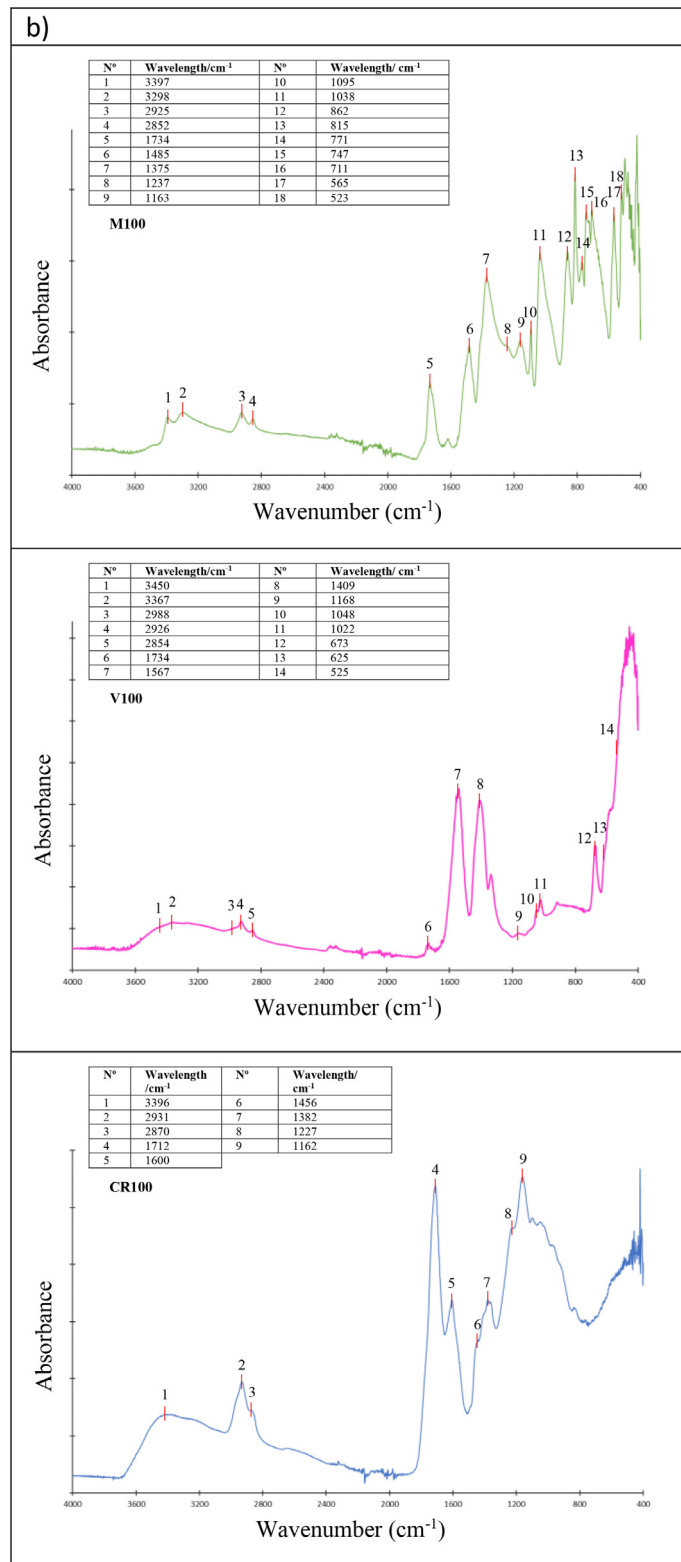


Fig. 5. Continued

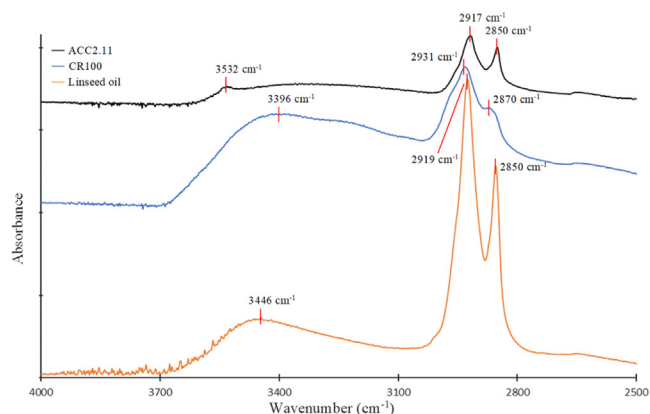


Fig. 6. IR spectra from ACC2.11 sample and both references (linseed oil and copper resin aged), in the range of 2500 and 4000 cm^{-1} .

tunic (ACC5.3) showed a mixture of copper resin and/or verdigris with a few particles of malachite, while in the mixture, while in the mixture used for the landscape leaves ACC5.13 the presence of malachite was more evident.

Acknowledgements

We acknowledge the financial support from the research groups FQM-338 and HUM-839. Funding for open access charge: University of Granada / CBUA.

Supplementary materials

Supplementary material associated with this article can be found, in the online version, at doi:[10.1016/j.culher.2022.12.004](https://doi.org/10.1016/j.culher.2022.12.004).

References

- [1] H. Kühn, *Verdigris and copper resinate, Artists' Pigments: a Handbook of Their History and Characteristics*, Oxford University Press, New York, 2008.
- [2] R.J. Gettens, E.W. Fitzhugh, Malachite and green verditer, *Stud. Conserv.* 19 (1) (1974) 2–23, doi:[10.1179/sic.1974.001](https://doi.org/10.1179/sic.1974.001).
- [3] J. Buse, V. Otero, M.J. Melo, New insights into synthetic copper greens: the search for specific signatures by Raman and Infrared spectroscopy for their characterization in Medieval artworks, *Herit* 2 (2) (2019) 1614–1629, doi:[10.3390/heritage2020099](https://doi.org/10.3390/heritage2020099).
- [4] E. Platania, N.L.W. Streeton, A. Lluveras-Tenorio, A. Vila, D. Buti, F. Caruso, H. Kutzke, A. Karlsson, M.P. Colombini, E. Uggerud, Identification of green pigments and binders in late medieval painted wings from Norwegian churches, *Microchem. J.* 156 (2020) 104811, doi:[10.1016/j.microc.2020.104811](https://doi.org/10.1016/j.microc.2020.104811).
- [5] A. Palomino, *El Museo pictórico y Escala Óptica II. Práctica De La Pintura*, Aguilar, Madrid, 1988, p. 528. <http://hdl.handle.net/20.500.11938/77542>
- [6] N. Navas, J. Romero-Pastor, E. Manzano, C. Cardell, Raman spectroscopic discrimination of pigments and tempera paint model samples by principal component analysis on first-derivative spectra, *J. Raman Spectrosc.* 41 (11) (2010) 1486–1493, doi:[10.1002/jrs.2646](https://doi.org/10.1002/jrs.2646).
- [7] E. Manzano, J. García-Atero, A. Dominguez-Vidal, M.J. Ayora-Cañada, L.F. Capitán-Vallvey, N. Navas, Discrimination of aged mixtures of lipidic paint binders by Raman spectroscopy and chemometrics, *J. Raman Spectrosc.* 43 (6) (2012) 781–786, doi:[10.1002/jrs.3082](https://doi.org/10.1002/jrs.3082).
- [8] A. Coccato, D. Bersani, A. Coudray, J. Sanyova, L. Moens, P. Vandenberghe, Raman spectroscopy of green minerals and reaction products with an application in Cultural Heritage research, *J. Raman Spectrosc.* 47 (12) (2016) 1429–1443, doi:[10.1002/jrs.4956](https://doi.org/10.1002/jrs.4956).
- [9] B. Gilbert, S. Denoël, G. Weber, D. Allart, Analysis of green copper pigments in illuminated manuscripts by micro-Raman spectroscopy, *Anal* 128 (10) (2003) 1213–1217, doi:[10.1039/B306138H](https://doi.org/10.1039/B306138H).
- [10] C. Conti, J. Striova, I. Aliatis, E. Possenti, G. Massonnet, C. Muehlethaler, M. Positano, The detection of copper resinate pigment in works of art: contribution from Raman spectroscopy, *J. Raman Spectrosc.* 45 (11–12) (2014) 1186–1196, doi:[10.1002/jrs.4455](https://doi.org/10.1002/jrs.4455).
- [11] S. Vahur, A. Teearu, I. Leito, ATR-FT-IR spectroscopy in the region of 550–230 cm^{-1} for identification of inorganic pigments, *Spectrochim. Acta Part A* 75 (3) (2010) 1061–1072, doi:[10.1016/j.saa.2009.12.056](https://doi.org/10.1016/j.saa.2009.12.056).

- [12] P. Richardin, V. Mazel, P. Walter, O. Laprévotte, A. Brunelle, Identification of different copper green pigments in renaissance paintings by cluster-TOF-SIMS imaging analysis, *J. Am. Soc. Mass Spectrom.* 22 (10) (2011) 1729–1736, doi:[10.1007/s13361-011-0171-3](https://doi.org/10.1007/s13361-011-0171-3).
- [13] A. Duran, M.C. Jimenez de Haro, J.L. Perez-Rodriguez, M.L. Franquelo, L.K. Herrera, A. Justo, Determination of pigments and binders in Pompeian Wall paintings using synchrotron radiation - high-resolution X-Ray powder diffraction and conventional spectroscopy - chromatography, *Archaeometry* 52 (2010) 286–307, doi:[10.1111/j.1475-4754.2009.00478.x](https://doi.org/10.1111/j.1475-4754.2009.00478.x).
- [14] J.S. Pozo-Antonio, D. Barral, A. Herrera, K. Elert, T. Rivas, C. Cardell, Effect of tempera paint composition on their superficial physical properties- application of interferometric profilometry and hyperspectral imaging techniques, *Prog. Org. Coat.* 117 (2018) 56–68, doi:[10.1016/j.porgcoat.2018.01.007](https://doi.org/10.1016/j.porgcoat.2018.01.007).
- [15] M. Breitman, S. Ruiz-Moreno, A.L. Gil, Experimental problems in Raman spectroscopy applied to pigment identification in mixtures, *Spectrochim. Acta Part A* 68 (4) (2007) 1114–1119, doi:[10.1016/j.saa.2007.06.042](https://doi.org/10.1016/j.saa.2007.06.042).
- [16] M. Gunn, G. Chottard, E. Rivière, J.J. Girerd, J.C. Chottard, Chemical reactions between copper pigments and oleoresinous media, *Stud. Conserv.* 47 (1) (2002) 12–23, doi:[10.1179/sic.2002.47.1.12](https://doi.org/10.1179/sic.2002.47.1.12).
- [17] L. Lepot, K. De Wael, F. Gason, B. Gilbert, G. Eppe, C. Malherbe, Discrimination of textile dyes in binary mixtures by Raman spectroscopy, *J. Raman Spectrosc.* 51 (2020) 717–730, doi:[10.1002/jrs.5831](https://doi.org/10.1002/jrs.5831).
- [18] J.J. González-Vidal, R. Perez-Pueyo, M.J. Soneira, S. Ruiz-Moreno, Automatic identification system of Raman spectra in binary mixtures of pigments, *J. Raman Spectrosc.* 43 (11) (2012) 1707–1712, doi:[10.1002/jrs.4177](https://doi.org/10.1002/jrs.4177).
- [19] P.A. Hayes, S. Vahur, I. Leito, ATR-FTIR spectroscopy and quantitative multivariate analysis of paints and coating materials, *Spectrochim. Acta Part A* 133 (2014) 207–213, doi:[10.1016/j.saa.2014.05.058](https://doi.org/10.1016/j.saa.2014.05.058).
- [20] P. Giménez, A. Linares, C. Sessa, H. Hagán, J.F. García, Capability of Far-Infrared for the selective identification of red and black pigments in paint layers, *Spectrochim. Acta Part A* 266 (2022) 120411, doi:[10.1016/j.saa.2021.120411](https://doi.org/10.1016/j.saa.2021.120411).
- [21] A.M. Gueli, S. Gallo, S. Pasquale, Optical and colorimetric characterization on binary mixtures prepared with coloured and white historical pigments, *Dye. Pigment.* 157 (2018) 342–350, doi:[10.1016/j.dyepig.2018.04.068](https://doi.org/10.1016/j.dyepig.2018.04.068).
- [22] D. Fontana, M.F. Alberghina, R. Barraco, S. Basile, L. Tranchina, M. Brai, S.O. Troja, Historical pigments characterisation by quantitative X-ray fluorescence, *J. Cult. Herit.* 15 (3) (2014) 266–274, doi:[10.1016/j.culher.2013.07.001](https://doi.org/10.1016/j.culher.2013.07.001).
- [23] C. Sessa, H. Bagán, J.F. García, Evaluation of MidIR fibre optic reflectance: detection limit, reproducibility and binary mixture discrimination, *Spectrochim. Acta Part A* 115 (2013) 617–628, doi:[10.1016/j.saa.2013.06.088](https://doi.org/10.1016/j.saa.2013.06.088).
- [24] G. Dupuis, M. Menu, Quantitative characterisation of pigment mixtures used in art by fibre-optics diffuse-reflectance spectroscopy, *Appl. Phys.* 83 (2006) 469–474, doi:[10.1007/s00339-006-3522-3](https://doi.org/10.1007/s00339-006-3522-3).
- [25] J.Y. Roh, M.K. Matecki, S.A. Svoboda, K.L. Wustholz, Identifying pigment mixtures in art using SERS: a treatment flowchart approach, *Anal. Chem.* 88 (4) (2016) 2028–2032, doi:[10.1021/acs.analchem.6b00044](https://doi.org/10.1021/acs.analchem.6b00044).
- [26] P.M. Ramos, J. Ferré, I. Ruisánchez, K.S. Andrikopoulos, Fuzzy logic for identifying pigments studied by Raman spectroscopy, *Appl. Spectrosc.* 58 (7) (2004) 848–854 <https://opg.optica.org/abstract.cfm?URL=as-58-7-848>.
- [27] D. Buti, F. Rosi, B.G. Brunetti, C. Miliani, In-situ identification of copper-based green pigments on paintings and manuscripts by reflection FTIR, *Anal. Bioanal. Chem.* 405 (2013) 2699–2711, doi:[10.1007/s00216-013-6707-6](https://doi.org/10.1007/s00216-013-6707-6).
- [28] M. San Andrés, J.M. De la Roja, V.G. Baonza, N. Sancho, Verdigris pigment: a mixture of compounds. Input from Raman spectroscopy, *J. Raman Spectrosc.* 41 (11) (2010) 1468–1476, doi:[10.1002/jrs.2786](https://doi.org/10.1002/jrs.2786).
- [29] N. Salvadó, T. Pradell, E. Pantos, M.Z. Papiz, J. Molera, M.E. Seco, M. Vendrell-Saz, Identification of copper-based green pigments in Jaume Huguet's Gothic altarpieces by Fourier transform infrared microspectroscopy and synchrotron radiation X-ray diffraction, *J. Synchrotron Radiat.* 9 (4) (2002) 215–222, doi:[10.1107/S0909049502007859](https://doi.org/10.1107/S0909049502007859).
- [30] E. Manzano, L.R. Rodríguez-Simón, N. Navas, Capitán-Vallvey, Non-Invasive and Spectroscopic Techniques for the Study of Alonso Cano's Visitation from the Golden Age of Spain, *Stud. Conserv.* 66 (5) (2021) 298–312, doi:[10.1080/00393630.2020.1830528](https://doi.org/10.1080/00393630.2020.1830528).
- [31] E. Manzano, L.R. Rodríguez-Simón, N. Navas, R. Checa-Moreno, M. Romero-Gómez, L.F. Capitán-Vallvey, Study of the GC-MS determination of the palmitic-stearic acid ratio for the characterisation of drying oil in painting: La Encarnación by Alonso Cano as a case study, *Talanta*, *J. Anal. Chem. New York* (2011) 1148–1154, doi:[10.1016/j.talanta.2011.03.012](https://doi.org/10.1016/j.talanta.2011.03.012).
- [32] A. Calvo Castellón, S. Gallego Miranda, in: *Aproximación Bibliográfica a Alonso Cano y Su Escuela*, 32, Cuadernos de Arte de la Universidad de Granada, 2001, pp. 377–400. <https://revistaseug.ugr.es/index.php/caug/article/view/9044>.
- [33] M.L. Franquelo, A. Duran, L.K. Herrera, M.J. De Haro, J.L. Perez-Rodriguez, Comparison between micro-Raman and micro-FTIR spectroscopy techniques for the characterization of pigments from Southern Spain Cultural Heritage, *J. Mol. Struct.* 924 (2009) 404–412, doi:[10.1016/j.molstruc.2008.11.041](https://doi.org/10.1016/j.molstruc.2008.11.041).
- [34] Infrared and Raman Users Group (IRUG database) <http://www.irug.org/search-spectral-database>. Accessed 21 June 2022.
- [35] I.M. Bell, R.J. Clark, P.J. Gibbs, Raman spectroscopic library of natural and synthetic pigments (pre-~ 1850 AD), *Spectrochim. Acta Part A* 53 (12) (1997) 2159–2179, doi:[10.1016/S1386-1425\(97\)00140-6](https://doi.org/10.1016/S1386-1425(97)00140-6).
- [36] M.C. Caggiani, A. Cosentino, A. Mangano, Pigments Checker version 3.0, a handy set for conservation scientists: a free online Raman spectra database, *Microchem. J.* 129 (2016) 123–132, doi:[10.1016/j.microc.2016.06.020](https://doi.org/10.1016/j.microc.2016.06.020).
- [37] A. Coccato, L. Moens, P. Vandenberghe, On the stability of mediaeval inorganic pigments: a literature review of the effect of climate, material selection, bio-

- logical activity, analysis, and conservation treatments, *Hérit. Sci.* 5 (1) (2017) 1–25, doi:[10.1186/s40494-017-0125-6](https://doi.org/10.1186/s40494-017-0125-6).
- [38] T.D. Chaplin, R.J. Clark, D.A. Scott, Study by Raman microscopy of nine variants of the green–blue pigment Verdigris, *J. Raman Spectrosc.* 37 (1) (2006) 223–229–3, doi:[10.1002/jrs.1469](https://doi.org/10.1002/jrs.1469).
- [39] F.C. Izzo, E. Zendri, A. Bernardi, E. Balliana, M. Sgobbi, The study of pitch via gas chromatography-mass spectrometry and Fourier-transformed infrared spectroscopy: the case of the Roman amphoras from Monte Poro, Calabria (Italy), *J. Archaeol. Sci.* 40 (1) (2013) 595–600, doi:[10.1016/j.jas.2012.06.017](https://doi.org/10.1016/j.jas.2012.06.017).
- [40] V. Otero, D. Sanches, C. Montagner, M. Vilarigues, L. Carlyle, J.A. Lopes, M.J. Melo, Characterisation of metal carboxylates by Raman and infrared spectroscopy in works of art, *J. Raman Spectrosc.* 45 (2014) 1197–1206, doi:[10.1002/jrs.4520](https://doi.org/10.1002/jrs.4520).
- [41] V. Beltran, N. Salvadó, S. Butí, G. Cinque, Micro infrared spectroscopy discrimination capability of compounds in complex matrices of thin layers in real sample coatings from artworks, *Microchem. J.* 118 (2015) 115–123, doi:[10.1016/j.microc.2014.09.001](https://doi.org/10.1016/j.microc.2014.09.001).